

Supporting Information

Couto et al. 10.1073/pnas.1201232109

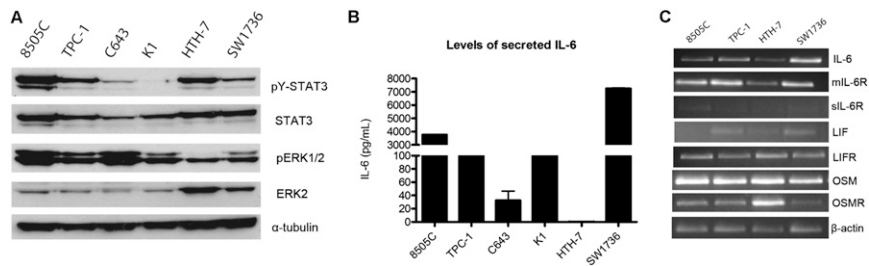


Fig. S1. (A) STAT3 Y705 phosphorylation (pY-STAT3) is heterogeneously expressed in thyroid cancer-derived cell lines (TCCs). Total extracts from the indicated TCCs were probed with the indicated antibodies; α -tubulin was the loading control. (B) Levels of IL-6 present in serum-free conditioned medium from the indicated TCCs were measured by ELISA (mean \pm SD). (C) RT-PCR showing RNA levels of *IL-6*, leukemia inhibitory factor (LIF), and oncostatin M as well as their receptors [membrane *IL-6* receptor, soluble *IL-6* receptor, LIF receptor, and oncostatin M receptor, respectively] in TCCs. β -actin was used for normalization.

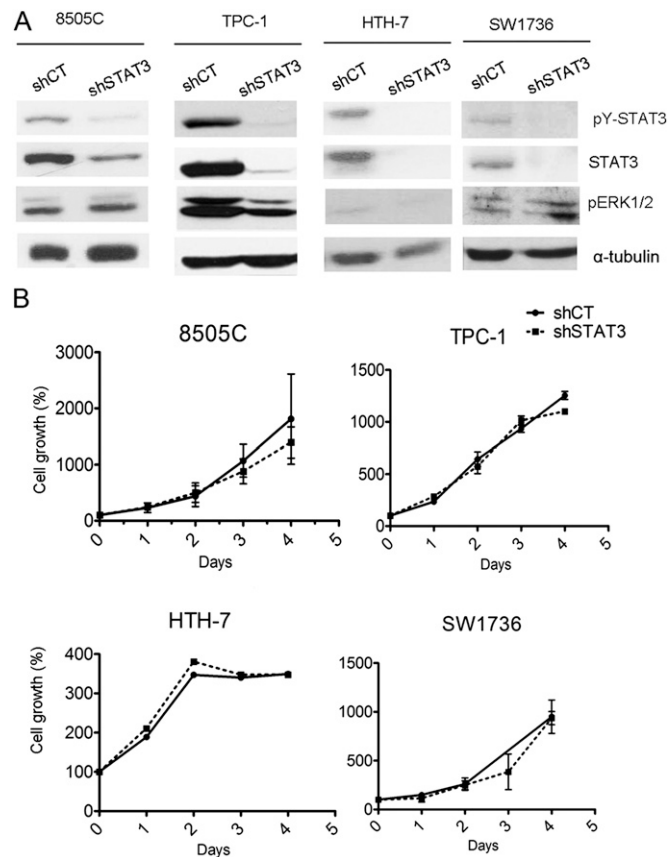


Fig. S2. STAT3 knockdown in thyroid cancer cell lines does not alter in vitro cell growth. (A) Extracts from 8505C, TPC-1, HTH-7, and SW1736 cell lines stably transfected with control lentivirus short hairpin control (shCT) and a lentivirus containing a short hairpin targeting STAT3 (shSTAT3) were analyzed by Western blotting for pY-STAT3, STAT3, pERK1/2, and α -tubulin. (B) Proliferation of shSTAT3 and shCT expressing cell lines was determined by Calcein AM quantification daily over 4 d.

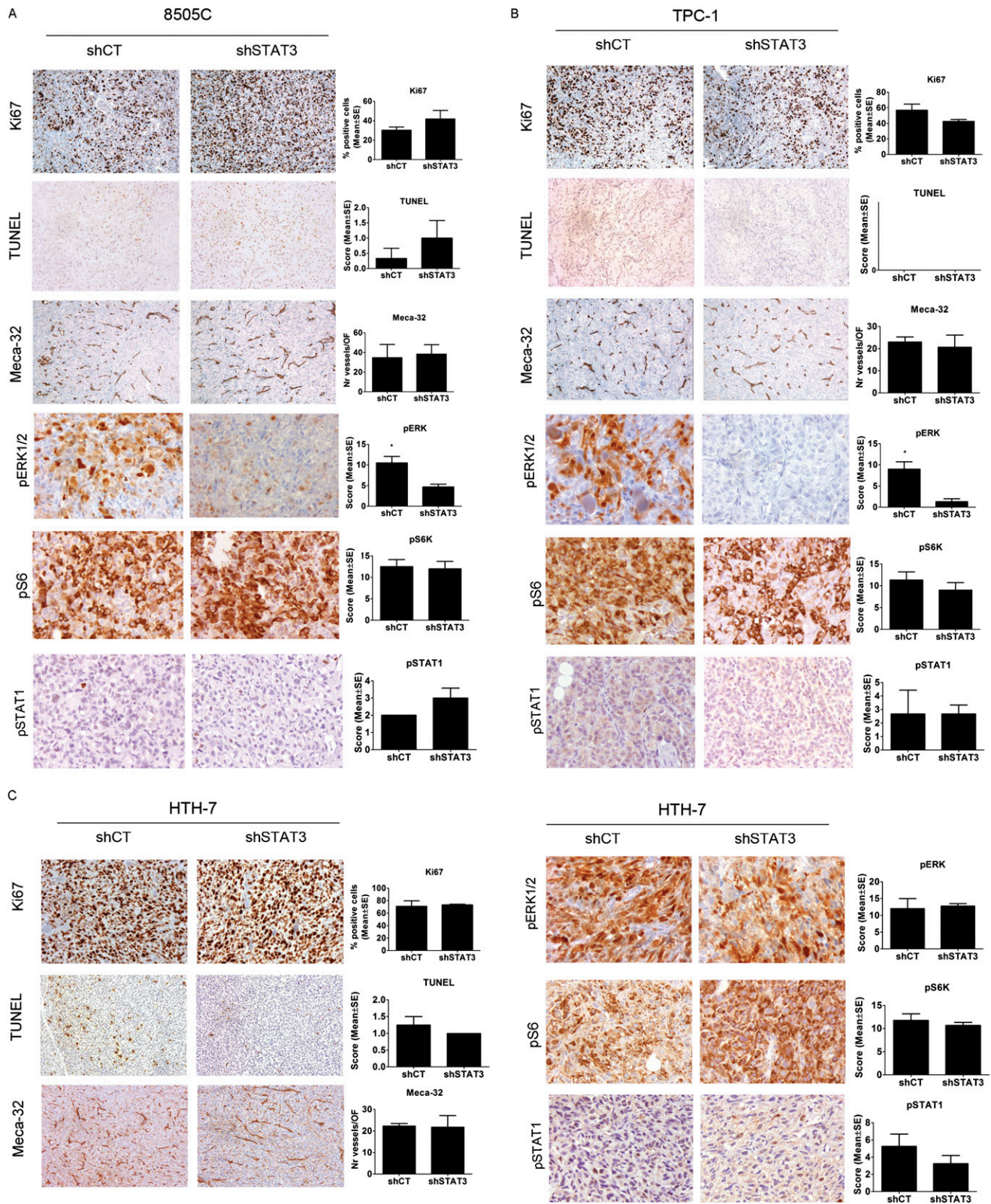


Fig. S3. shSTAT3 tumors do not show a significant increase in proliferation, apoptosis, and angiogenesis. Sections from 8505C (A), TPC-1 (B), and HTH-7 (C) shCT and shSTAT3 tumors were immunostained for markers of proliferation (protein Ki67), apoptosis (TUNEL), and angiogenesis (Meca-32) as well as pERK1/2 (*t* test $P < 0.05$), pS6, and pSTAT1. Quantification is represented on the right. (Magnification: 200 \times .) * $P < 0.05$.

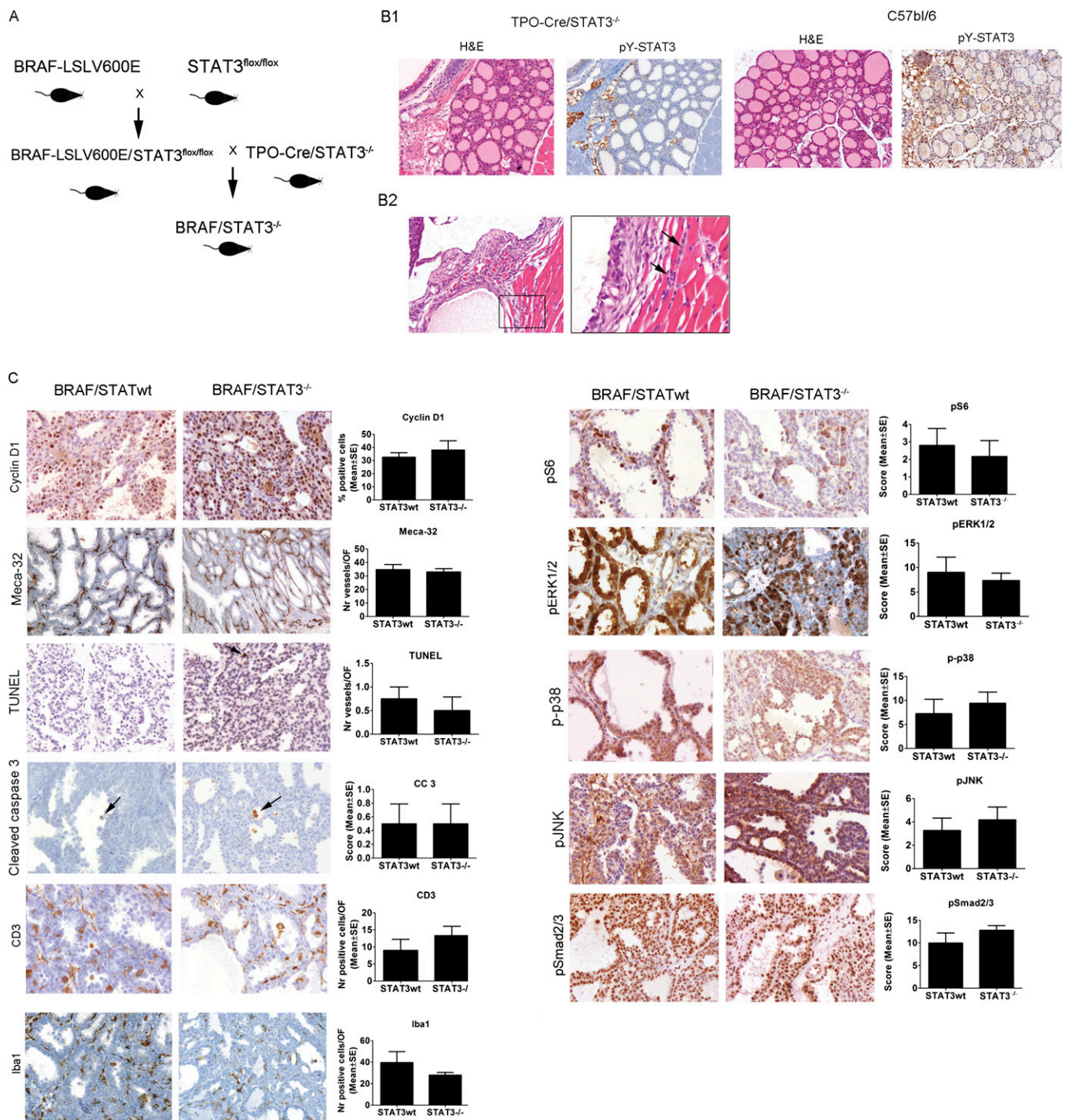


Fig. 55. (A) Schematic representation of v-RAF murine sarcoma viral oncogene homolog B (BRAF)/STAT3^{-/-} mice generation. (B, 1) STAT3 deficiency in normal thyrocytes does not alter thyroid histological morphology. Representative H&Es and pY-STAT3 staining of the thyroid glands from 5-wk-old thyroid peroxidase-Cre/STAT3^{-/-} and 5-wk-old C57Bl/6 WT mice. (B, 2) At 5 wk of age, both STAT3wt and STAT3^{-/-} mice showed skeletal muscle invasion (arrows). (C) Representative sections from BRAF/STAT3wt STAT3^{-/-} mice were immunostained for the expression of markers of proliferation (cyclin D1), angiogenesis (Meca-32), apoptosis (TUNEL/cleaved-caspase 3), T cells (CD3), and macrophages (Iba1) as well as the activation of v-akt murine thymoma viral oncogene homolog 1 (AKT) (pS6), MAPK (pERK, p-p38, and pJNK), and TGF- β (pSmad2/3) signaling. (Magnification: 200 \times ; Meca-32, 100 \times .) Quantification of at least six different animals is represented in the bar graphs (mean \pm SEM).

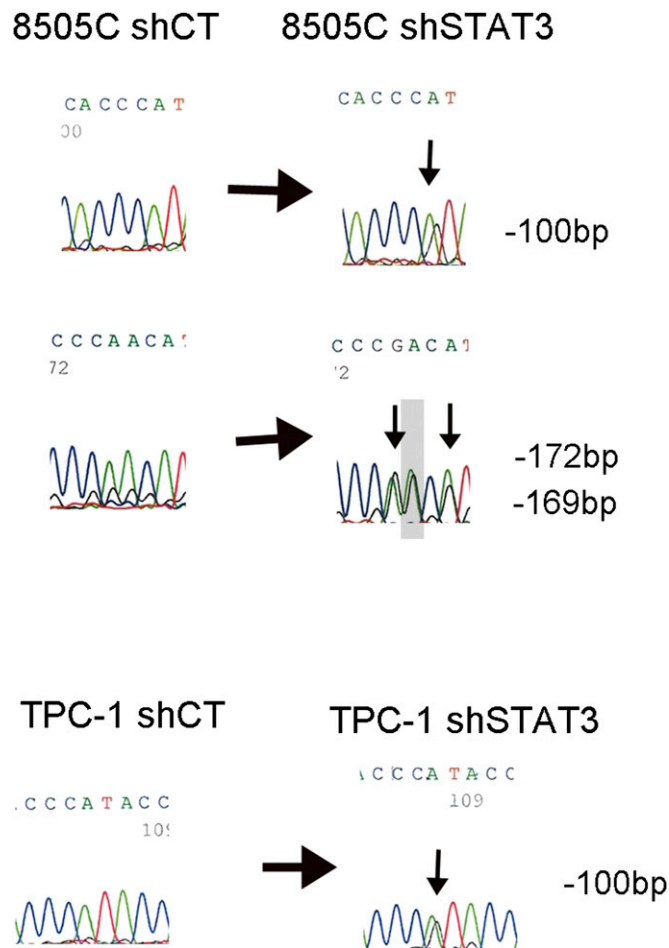


Fig. S6. shSTAT3 TCCs show additional cytosine methylation of the *insulin-like growth factor binding protein 7 (IGFBP7)* promoter. Bisulfite sequencing (reverse strand) of the -237- to +10-bp region of the *IGFBP7* promoter in 8505C and TPC-1 shCT and shSTAT3 cell lines. Arrows point at partially methylated cytosines (reverse is G), and numbers indicate their location in the promoter. The gray bar represents a polymorphic site.

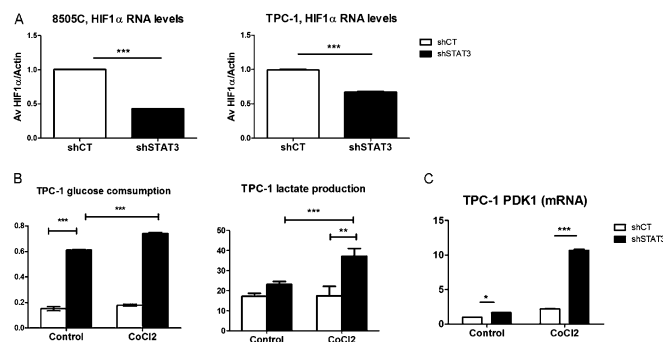


Fig. S7. *HIF1A* RNA levels, glucose uptake, lactate production and *PDK1* RNA levels in TPC-1 shCT and shSTAT3 cell lines treated with cobalt chloride (100 μ m) for 24 hours. (A) *HIF1A* RNA levels were determined by Taqman RT-PCR and normalized to β -actin. Bars are mean \pm SEM, $n = 3$. (B) Glucose uptake was determined by subtracting the glucose concentration in the supernatant to the initial concentration in fresh medium RPMI. Lactate was measured in cell's supernatant. Results were normalized to protein amount (milligrams). Bars represent mean \pm SEM, $n = 3$. (C) *PDK1* RNA levels were determined by Taqman RT-PCR and normalized to β -actin. Bars are mean \pm SEM, $n = 3$. * $P < 0.05$, ** $P < 0.01$, *** $P < 0.0001$.

Table S1. Summary of the genetic alterations present in ERK/MAPK signaling effectors in the TCCs used in this study (1, 2)

Cell line	Original lesion	RAS	RET	BRAF
8505C	Undifferentiated thyroid carcinoma	WT	WT	V600E
TPC-1	Papillary thyroid carcinoma	WT	RET/PTC1	WT
C643	Undifferentiated thyroid carcinoma	HRAS G13R	WT	WT
K1	Papillary thyroid carcinoma	WT	WT	V600E
HTH-7	Undifferentiated thyroid carcinoma	NRAS Q61R	WT	WT
SW1736	Undifferentiated thyroid carcinoma	WT	WT	V600E

BRAF, v-RAF murine sarcoma viral oncogene homolog B; HRAS, v-Ha-ras Harvey rat sarcoma viral oncogene homolog; NRAS, neuroblastoma RAS viral (v-ras) oncogene homolog; PTC is not written in this table. RAS, rat sarcoma virus oncogene; RET, rearranged during transfection; cell line SW1736.

1. Meireles AM, et al. (2007) Molecular and genotypic characterization of human thyroid follicular cell carcinoma-derived cell lines. *Thyroid* 17:707–715.
2. Ricarte-Filho JC, et al. (2009) Mutational profile of advanced primary and metastatic radioactive iodine-refractory thyroid cancers reveals distinct pathogenetic roles for BRAF, PIK3CA, and AKT1. *Cancer Res* 69:4885–4893.

Table S2. Differentially expressed genes between shCT and shSTAT3 cell lines that were identified by genome expression analysis

Genes	Variation	Cell lines
Inflammation		
Chemokine (C-C motif) ligand 2	Down-regulated	8505C; HTH-7
IL-13 receptor, α -2	Down-regulated	8505C; HTH-7
TNF receptor superfamily, member 21	Down-regulated	8505C; HTH-7
Growth factor signaling		
IGFBP7	Down-regulated	8505C; HTH-7
TGF, β -receptor II	Down-regulated	8505C; HTH-7
Extracellular matrix		
EGF-containing fibulin-like extracellular matrix protein 1	Down-regulated	8505C; TPC-1; HTH-7
Collagen, type V, α -1	Down-regulated	8505C; HTH-7
Matrix metalloproteinase 3	Up-regulated	8505C; HTH-7

The list is restricted to genes with expression that was altered in the same direction in at least two of the cell lines.

Dataset S1. List of differentially regulated genes in shSTAT3 vs. shCT thyroid cancer cell lines ($P < 0.05$)

[Dataset S1](#)